PROCEEDINGS OF SCIENCE

New results for searches of exotic decays with NA62 in beam-dump mode

Jan Jerhot*

Université Catholique de Louvain,
Center for Cosmology, Particle Physics and Phenomenology,
Chemin du Cyclotron 2, Louvain-la-Neuve, Belgium

E-mail: jan.jerhot@cern.ch

We report on the search for visible decays of exotic mediators from data taken in "beam-dump" mode with the NA62 experiment. The NA62 experiment can be run as a "beam-dump experiment" by removing the kaon production target and dumping the proton beam in closed collimators. More than 10^{17} protons on target have been collected in this way during a week-long data-taking campaign by the NA62 experiment. We report on new results from analysis of this data, with a particular emphasis on dark photon and axion-like particle models.

21st Conference on Flavor Physics and CP Violation
29 May - 2 June 2023
IP2I - Lyon University, Lyon, France

*On behalf of the NA62 Collaboration.

PoS(FPCP2023)073

1. Introduction

Fixed-target experiments offer a complementary approach to collider experiments in search for New Physics (NP) particles. While most of the collider experiments focus on directly probing mass scales around $O(1)$ TeV, so-called energy frontier, fixed-target experiments operate at lower center of mass energies. Despite the lower energies, fixed-target experiments have the advantage of collecting a large amount of data with well-controlled background, known as the intensity frontier.

At the intensity frontier, fixed-target experiments indirectly probe very large mass scales ($\gtrsim$ 100 TeV) through precise measurements of Standard Model (SM) processes and searches for decays that are forbidden in the SM. Additionally, they directly probe smaller mass scales ranging from $O(1)$ MeV to $O(1)$ GeV for very small couplings C_X of NP particles to the SM particles.

The range of m_X and C_X that can be directly probed by fixed-target experiments is particularly interesting in models describing hypothetical mediators between Dark Matter (DM) and SM particles, collectively referred to as Dark Sector portals. These mediators not only facilitate interactions between the SM and the DM sector but also offer potential explanations for various observations that are not accounted for by the SM, such as neutrino masses and the hierarchy of SM masses.

The following table summarizes four portals corresponding to the main benchmark scenarios of the Physics Beyond Colliders initiative [1] and corresponding SM final states that can be searched for in NP particle decays at fixed-target experiments. Details of the fields and coupling constants involved will be given in dedicated sections.

Table 1: *Dark Sector portals.*

NP Particle	type	Dark Sector portal (dim $\leq$ 5)	decay ($m \lesssim 1$ GeV)
dark photon (A'_μ)	vector	$-\frac{\varepsilon}{2\cos\theta_W} F'_{\mu\nu} B^{\mu\nu}$	$\ell\ell$, $\pi\pi$, $\pi\pi\pi$
axion/ALP[1] (a)	pseudoscalar	$\frac{C_{VV}}{\Lambda} a V_{\mu\nu}\tilde{V}^{\mu\nu}$, $\frac{C_{ff}}{\Lambda}\partial_\mu a \bar{f}\gamma^\mu\gamma^5 f$	$\gamma\gamma$, $\ell\ell$, $2\pi\gamma$, 3π, $2\pi\eta$
HNL[2] (N_I)	fermion	$F_{\alpha I}(\bar{L}_\alpha H) N_I$	$\pi\ell(\nu)$,$\ell_1\ell_2(\nu)$
dark Higgs (S)	scalar	$(\mu S + \lambda S^2) H^\dagger H$	$\ell\ell$, $\pi\pi$

These new states can be searched for directly at fixed-target facilities in two types of processes:

- the decay of a NP particle into SM final states seen by the detector, which allows the reconstruction of the original NP particle;
- the decay of a SM particle into SM and NP particles where the NP particles can by reconstructed from the knowledge of the SM initial and final states even if the NP particle does not decay back to SM final states and escapes detection.

In the following sections we will focus on the first category of processes searched for at the NA62 experiment operated in *beam-dump mode*. NA62 can also perform searches for the second category of processes in the standard (*kaon*) mode through decays of kaons to NP particles. We

[1] Axion-like particle.
[2] Heavy neutral lepton.

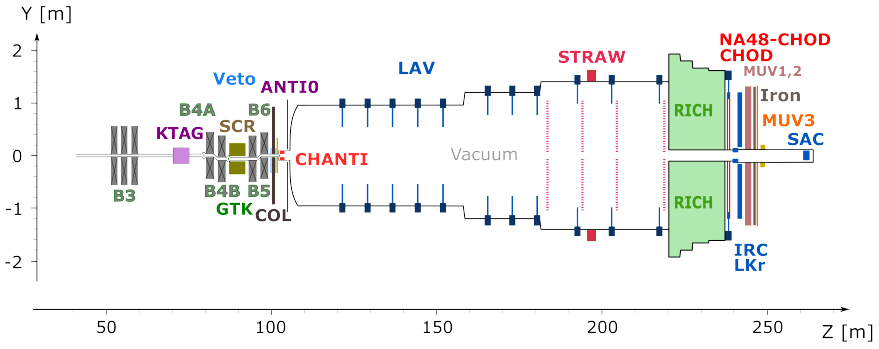

Figure 1: Schematic layout of the NA62 experiment in the Y-Z plane.

will present recent results concerning the search for the dark photon portal, and additionally outline advancements in investigating other portals and show future prospects.

2. NA62 experiment

The NA62 experiment is a fixed-target experiment at the CERN North Area and is served with a 400 GeV/c proton beam from the SPS. NA62 is a multi-purpose experiment covering a broad kaon and beam-dump physics programme with the main goal of measuring the branching ratio of the very rare $K^+ \to \pi^+\nu\bar{\nu}$ decay with 10% precision. About 4×10^{12} kaon decays have been collected during the data-taking period 2016-2018 (Run 1) and the result of the corresponding $\mathcal{B}_{K^+\to\pi^+\nu\bar{\nu}}$ measurement is $\mathcal{B}_{K^+\to\pi^+\nu\bar{\nu}} = (10.6 \pm 4.0) \times 10^{-11}$ [2]. Data-taking resumed in 2021 (Run 2) after the CERN Long Shutdown 2 (LS2).

2.1 Kaon mode

In standard data-taking mode, called the *kaon mode*, the 400 GeV/c proton beam impinges on a beryllium target, producing a secondary beam from which a 75 GeV/c component is selected using movable copper-iron collimators called TAXes, located about 23 m from the target. The 75 GeV/c secondary beam has a $\sim$ 750 MHz particle rate and consists of about 6% K^+. The kaons in the beam are selected using a Cherenkov counter detector (KTAG), which also provides the timing for the kaon tracks, while their momenta are measured by a silicon pixel spectrometer (GTK). The particle beam then enters a 117 m long vacuum vessel where about 14% of the beam kaons decay in the fiducial volume (FV) that occupies the first about 75 m of the vacuum vessel. The momenta of the kaon decay products are measured using the STRAW spectrometer, consisting of 4 straw stations and a 0.9 T·m magnet. The vacuum vessel is followed by a ring-imaging Cherenkov counter (RICH) optimized for the momentum range 15-35 GeV/c, to separate the final state π^+ and μ^+ [4]. Further particle identification (PID) is by a sequence of calorimeters: the electromagnetic calorimeter (LKr) and hadronic calorimeters (MUV1 and MUV2). Muon identification is provided by a scintillating-tile muon detector (MUV3), located behind an 80 cm thick iron wall. The RICH and the charged hodoscope (CHOD) also provide the timing for the tracks of the final state particles.

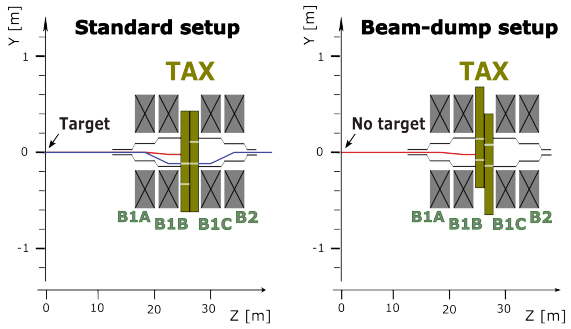

Figure 2: Schematic layout in the Y-Z plane of the NA62 experiment target area in the two modes of operation.

2.2 Beam-dump mode

When operated in the so-called *beam-dump mode* the NA62 experiment can search for NP particles too heavy to be produced in the kaon decays. In the beam-dump mode, the beryllium target is lifted from the beam line and the TAX collimators are closed, effectively dumping the 400 GeV/c beam. Only neutrinos, muons and hypothetical NP particles produced from the interaction of the beam with the material of the TAX and in secondary particle decays can penetrate the TAX and reach the NA62 decay volume. The currents of a set of dipole magnets, used for the modulation of the beam selected by TAX in the kaon mode, are set to produce magnetic fields in the same direction in the beam-dump mode in order to sweep the muons from the decay volume acceptance since the halo muon flux is the dominant background in the beam-dump mode [3]. The detectors preceding the decay volume are not used in the beam-dump data analyses except for an upstream veto (ANTI0), which allows further reduction of the muon halo background at the analysis level.

Three trigger lines are implemented in beam-dump mode:

1. Control, triggered by total deposited energy in the LKr of above 1 GeV and at least one reconstructed LKr cluster;
2. Q1/20, triggered by at least one signal in CHOD and downscaled by 20;
3. H2, triggered by two in-time signals in different CHOD tiles.

The low particle rate in beam-dump mode allows data to be collected at an increased proton beam intensity (about a factor 1.5 higher than in the kaon mode) resulting in rates of Control, Q1/20 and H2 triggers of 4, 14 and 16 kHz respectively.

In 2021, data from $(1.4 \pm 0.28) \times 10^{17}$ protons dumped on TAX (POT) were collected at NA62 during a period of 10 days of operation in the beam-dump mode. During the whole of Run 2 a total of about $N_{\mathrm{POT}} = 10^{18}$ POT is expected.

3. Search for dark photons

The dark photon A' is a vector particle corresponding to a new $U(1)$ gauge symmetry. In the "minimal scenario" the dark photon interacts with the SM hypercharge through a kinetic mixing

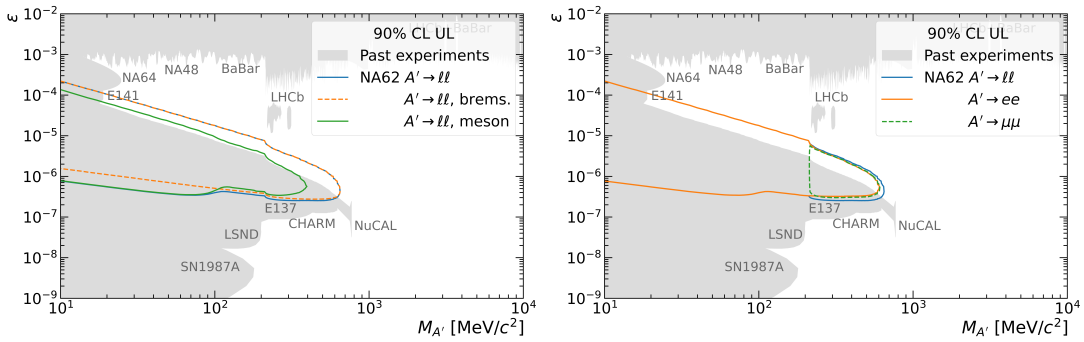

Figure 3: NA62 sensitivity to dark photons, assuming 0 observed events in 1.4×10^{17} POT, per production mechanism (left) and per decay mode (right).

term

$$\mathcal{L} \supset -\frac{\varepsilon}{2\cos\theta_W} F'_{\mu\nu} B^{\mu\nu}, \tag{1}$$

where $F'_{\mu\nu} = \partial_\mu A'_\nu - \partial_\nu A'_\mu$, $B_{\mu\nu}$ is the SM hypercharge field strength tensor, θ_W is the Weinberg angle and ε is the coupling constant.

Dark photons can be produced through two mechanisms in the beam-dump mode at NA62 in proton-nucleus interactions:

- bremsstrahlung production: $p + N \to X + A'$;
- meson-mediated production: $p + N \to X + M$, $M \to A' + \gamma(\pi^0)$, where $M \in \{\pi^0, \eta, \rho, \omega, ..\}$.

The two mechanisms differ in cross-section and the angle-momentum distribution of the radiated dark photons, see NA62 sensitivity in Fig. 3 left. For dark photon masses $M_{A'} < 700$ MeV, the decay width is dominated by the lepton-antilepton decays, see Fig. 3 right. The expected dark photon yield N_{exp} is given by

$$N_{\text{exp}} = N_{\text{POT}} \times \chi(pp \to A') \times \mathcal{B}(A' \to \ell^+\ell^-) \times P_{RD}(\varepsilon) \times A_{\text{acc}} \times A_{\text{trig}}, \tag{2}$$

where $\chi(pp \to A')$ is the dark photon emission probability, $\mathcal{B}(A' \to \ell^+\ell^-)$ is the branching ratio, P_{RD} is the probability to decay in the NA62 decay volume and A_{acc} (A_{trig}) is the signal selection (trigger) efficiency.

A search for dark photon decays to a $\mu^+\mu^-$ and e^+e^- pairs has been performed at NA62 with a sample with $N_{\text{POT}} = 1.4 \times 10^{17}$ selected using the H2 trigger in the beam-dump mode. The strategy for this analysis is to find the secondary $\ell^+\ell^-$ vertex in the decay volume and reconstruct the primary vertex as the point of closest distance of approach (min[CDA_{TAX}]) of the reconstructed A' track to the proton beam. The primary vertex is expected to lie near the beam impact point on the TAX, see Fig. 4 for the expected signal distribution around the interaction point for $\mu^+\mu^-$ (left) and e^+e^- (right). The signal region (SR) is selected as $\pm 3\sigma$ in each axis of the expected signal distribution and is kept blinded in the data until the analysis is finalized. For the $\mu^+\mu^-$ analysis the SR is defined as a box $\text{CDA}_{\text{TAX}} < 20$ mm and 6 m $< Z_{\text{TAX}} <$ 40 m. An improved SR of an ellipse centered at $\text{CDA}_{\text{TAX}} = 0$ and $Z_{\text{TAX}} = 23$ m is used for the e^+e^- analysis as this better captures the shape of the

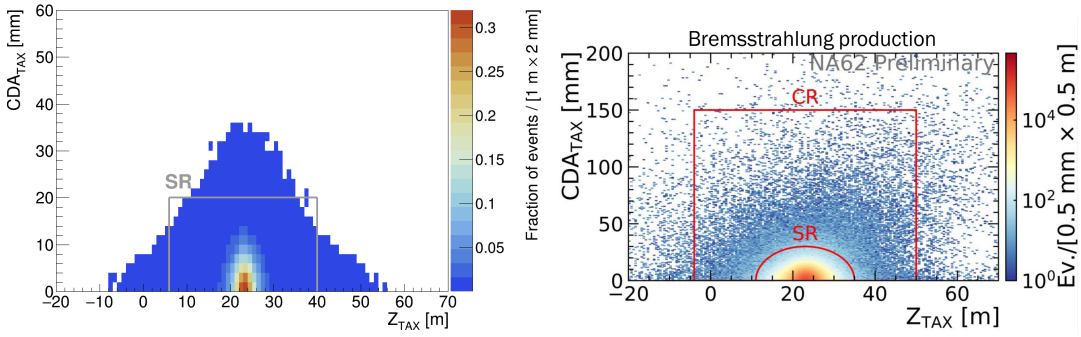

Figure 4: Signal MC and definition of control (CR) and signal regions (SR). Left: $\mu^+\mu^-$, right: e^+e^-.

distribution. The control region (CR) is defined in both analyses as a box $\mathrm{CDA_{TAX}} < 150$ mm and -4 m $< Z_{\mathrm{TAX}} < 50$ m.

For both analyses 2 tracks of opposite charge coincident in time with the trigger and with each other are required. The particle identification requires a single hit in MUV3 for each track and a ratio of energy deposited in the LKr and momentum $E/p < 0.2$ for the $\mu^+\mu^-$ analysis. For e^+e^- MUV3 is used as a veto instead and E/p is expected to be around 1. Additionally, no in-time activity in the LAV is allowed to reduce the background from secondary interactions of halo muons. For the e^+e^- analysis, the ANTI0 detector is used for further background suppression.

After applying the LAV veto, the dominant source of background in the $A' \to \mu^+\mu^-$ analysis is a random pairing of two halo muons from interactions of uncorrelated protons, so-called *combinatorial* background. To evaluate this background a control sample selected with the Q1 trigger in the absence of H2 has been used. The second background component is the so-called *prompt* background from secondary particles produced by interactions of halo muons. The prompt background has been simulated using backward MC simulation and unfolding techniques and the expected relative contribution to the $\mu^+\mu^-$ analysis after applying LAV veto has been evaluated as negligible (about 30% compared to the combinatorial). A good agreement between the expected and observed number of events in the $\mu^+\mu^-$ data sidebands is observed, see Fig.5 and Tab. 2.

In contrast, in the $A' \to e^+e^-$ analysis, the prompt background is the dominant background component and the combinatorial background is about an order of magnitude lower. A good

Table 2: Summary of expected $\mu^+\mu^-$ events from combinatorial background (N_{exp}), the related uncertainty (δN_{exp}), the observed events in data (N_{obs}) and the probability to obtain a likelihood L for data-MC compatibility equal or worse than that corresponding to N_{obs} ($P_{L\leq L_{\mathrm{obs}}}$).

	$N_{\mathrm{exp}} \pm \delta N_{\mathrm{exp}}$	N_{obs}	$p_{N\geq N_{\mathrm{obs}}}$	$p_{L\leq L_{\mathrm{obs}}}$
outside CR	26.3 ± 3.4	28	0.41	0.74
CR3	1.70 ± 0.22	2	0.25	0.25
CR2	0.58 ± 0.07	1	0.44	0.44
CR1	0.29 ± 0.04	1	0.50	0.68
CR1+2+3	2.57 ± 0.33	4	0.26	0.24

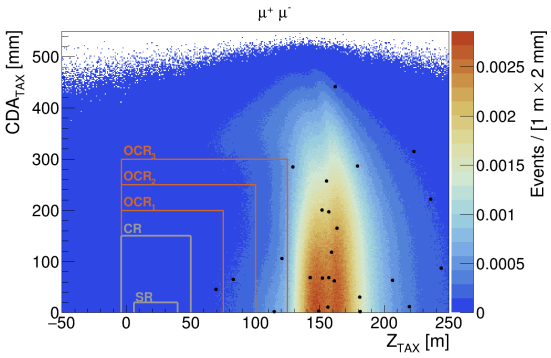

Figure 5: $\mu^+\mu^-$ MC (z-axis) - data (points) comparison, SR and CR closed.

agreement between the data and MC for the $A' \to e^+e^-$ sidebands is observed, see Fig.6, a remarkable result given the N_{POT}. Besides the SR and CR cuts, the combined LAV and ANTI0 veto provide an additional background suppression of almost 2 orders of magnitude.

After applying the full selection, the expected backgrounds in the signal and control regions are below 1 event in both analyses, see Tab.3.

Table 3: Summary of expected $\mu^+\mu^-$ and e^+e^- events in CR and SR at given confidence levels.

	$\mu^+\mu^-$@68% CL	e^+e^-@90% CL
CR	0.17 ± 0.02	$0.0097^{+0.0021}_{-0.007}$
SR	0.016 ± 0.002	$0.0094^{+0.0021}_{-0.007}$

After opening the control regions, no events were found in either decay channel. After opening the $\mu^+\mu^-$ SR, one event with invariant mass $\sim$ 411 MeV has been found. The corresponding upper limit at 90% CL is the region enclosed by black contour in Fig. 7 left. As a counting experiment, the global significance of the event observed is 2.4σ. Note, however, that the track time difference is about two standard deviations from the value of zero expected for in time tracks and that the extrapolation of the corresponding track to the impact point is barely in the SR, suggesting that the event found could be a combinatorial background event. After opening the e^+e^- SR, no events are found and the corresponding upper limit at 90% CL is the region enclosed by black contour in Fig. 7 right. The statistical combination of the two results is in progress.

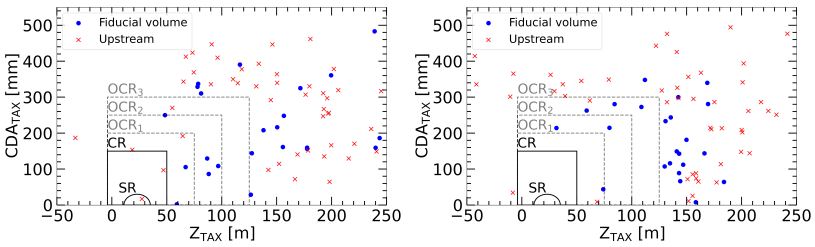

Figure 6: e^+e^- MC (left) - data (right) comparison, SR and CR closed.

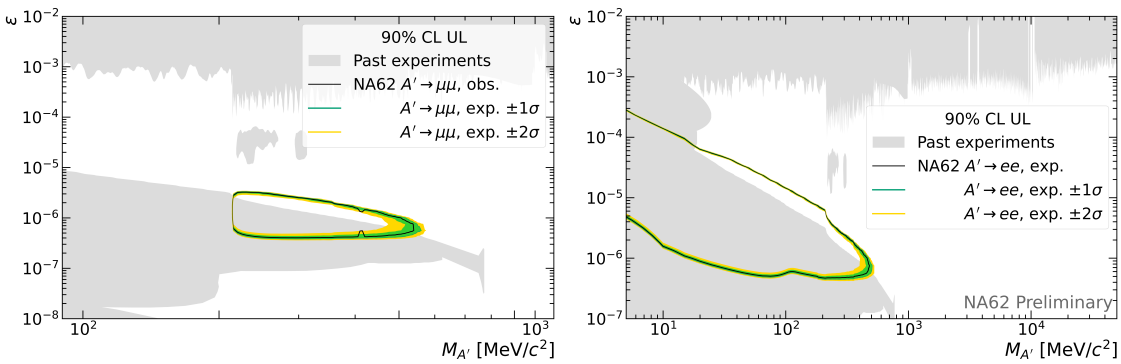

Figure 7: Final result with upper limit at 90% CL for $A' \to \mu^+\mu^-$ (left) and for $A' \to e^+e^-$ (right).

4. Search for axion-like particles

Axions were originally predicted as a possible explanation of CP conservation in strong interactions, called the Strong CP problem. A more general case with various possible couplings to the SM not necessarily addressing the strong CP problem (axion-like particle/ALP) is usually considered:

- SM gauge boson coupling: $\mathcal{L} \supset \dfrac{C_{VV}}{\Lambda} a V_{\mu\nu} \tilde{V}^{\mu\nu}, V \in \{B, W, G\}$;
- SM fermion coupling: $\mathcal{L} \supset \dfrac{C_{ff}}{\Lambda} \partial_\mu a \bar{f} \gamma^\mu \gamma^5 f, f \in \{q, \ell\}$.

If one of the ALP-SM couplings, C_{qq}, C_{gg}, C_{WW} is non-zero ALPs can be produced in flavour-changing neutral current decays, such as $B \to K^{(\star)} a$ and $K \to \pi a$. Depending on the coupling of ALPs to the SM, ALPs can be produced in the TAX in the beam-dump mode in various ways:

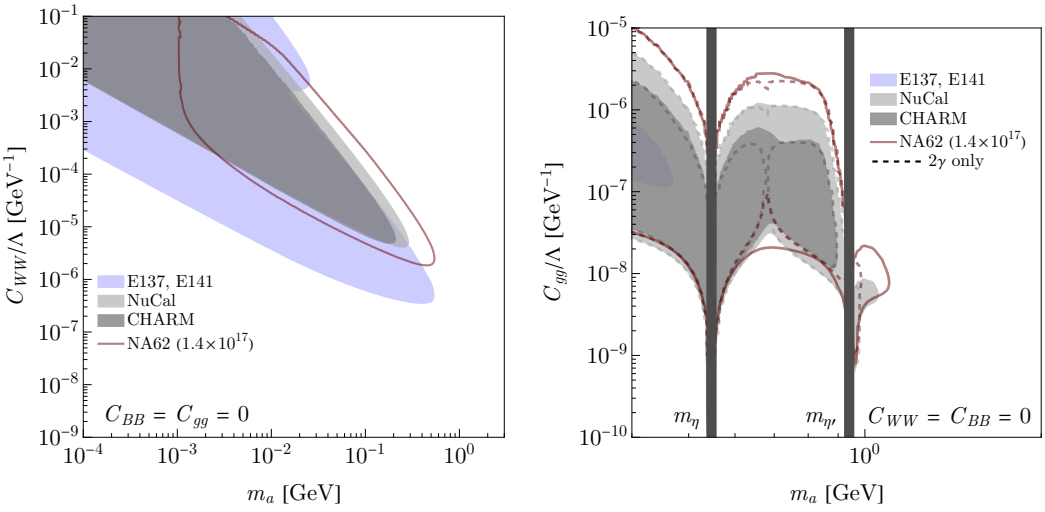

Figure 8: NA62 Run 2 sensitivity compared to previous exclusion limits. Left: $a \to 2\gamma$ search for C_{WW} coupled ALP. Right: $a \to$ hadrons and $a \to 2\gamma$ search for C_{gg} coupling-only [10].

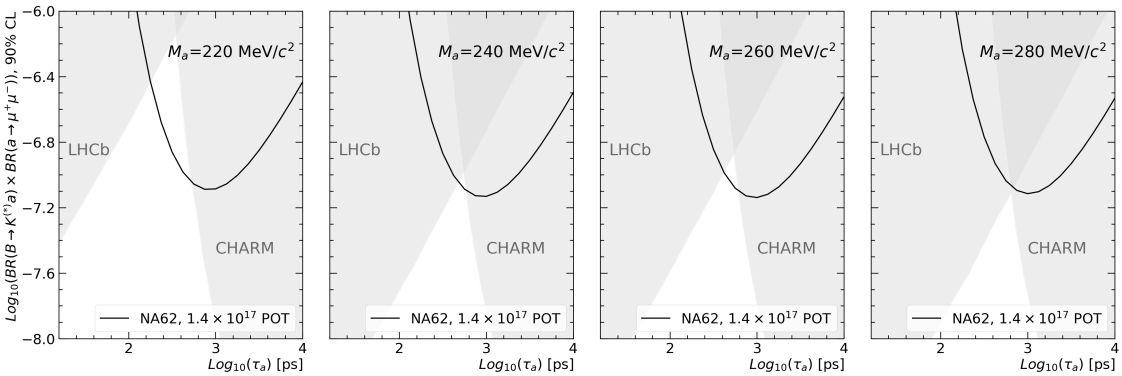

Figure 9: Resulting exclusion at 90% CL for ALP a with mass M_a and lifetime τ_a as a function of the product of the ALP production and decay branching ratios.

- photon-mediated (Primakoff) production from both off- and on-shell photons [7, 8];
- flavour-changing neutral current B meson decays [9];
- through mixing with other neutral pseudoscalars (π^0, η, η') [10];
- interaction of secondary muons with the TAX nuclei [11].

With the collected statistics of $(1.4 \pm 0.28) \times 10^{17}$ POT, NA62 is sensitive to various decay channels (di-photon, di-lepton, hadronic) of ALPs of masses and couplings that have not yet been probed by other experiments. See the NA62 sensitivity using a toy MC [10] Fig. 8 left for photonic coupling and right for gluonic coupling. The respective analyses with the current data sample are in progress.

The dark photon $A' \to \ell^+\ell^-$ decays would leave the same signature as a fermion-coupled ALP produced in TAX in a B meson decay and decaying in the decay volume to $\ell^+\ell^-$. See in Fig. 9 the result of the $A' \to \mu^+\mu^-$ analysis reinterpreted as a model-independent search for ALP.

5. Search for heavy neutral leptons

The general form of the HNL portal is

$$\mathcal{L} \supset F_{\alpha I}(\bar{L}_\alpha H)N_I, \tag{3}$$

where H is the Higgs doublet, L_α is the left-handed doublet of the SM neutrino of flavour α, N_I is the I-th HNL field and we sum over the flavour indices. Upon breaking the electroweak symmetry and diagonalizing the neutrino mass terms one obtains mixing terms between the neutrinos ν and HNLs L, typically parametrized by elements of matrix U for the respective flavours. Processes involving HNLs can then be obtained from the neutrino processes by an exchange $\nu_\alpha \to U_{\alpha I} L_I$.

At NA62 in the beam-dump mode, the dominant production is expected from decays of secondary D mesons in the TAX, for example $D \to \ell N$. See the expected sensitivity for minimal HNL scenarios for the full Run 2 statistics with a toy MC in Fig. 10 [5].

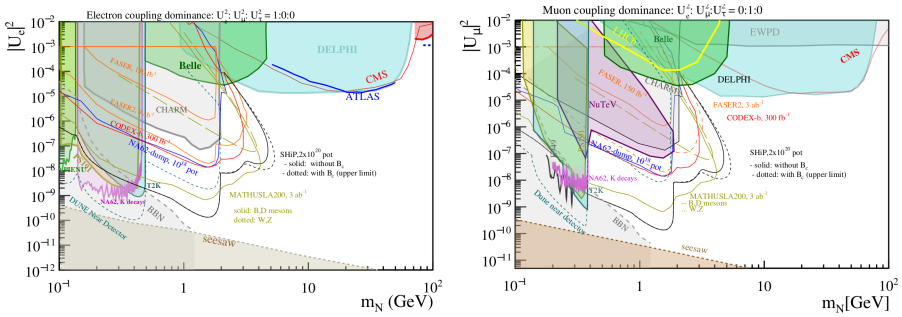

Figure 10: Upper limit at 90% CL on $|U_{\ell 4}|^2$ (left: $|U_{e4}|^2$, right: $|U_{\mu 4}|^2$) comparison with beam-dump searches. Blue contour: projected NA62 sensitivities at $N_{\mathrm{POT}} = 10^{18}$ combining searches for all kinematically allowed decay channels, including channels with open kinematics.

6. Search for dark Higgs

In the minimal model, a dark Higgs S is coupled to the SM Higgs boson through the $H^\dagger H$ operator as

$$\mathcal{L} \supset -(\mu S + \lambda S^2) H^\dagger H. \tag{4}$$

Below the electroweak symmetry breaking scale H is substituted by $(v+h)\sqrt{2}$ and non-zero coupling μ would lead to mixing between S and h, which can be parametrized for small μ as

$$\theta \simeq \theta = \frac{\mu v}{m_h^2 - m_S^2}, \tag{5}$$

where $v = 246$ GeV.

At loop level, the dark Higgs can be produced in flavour-changing neutral current processes, for example $B \to KS$ or $K \to \pi S$ decays. Therefore, dark Higgs can be produced in decays of secondary B mesons produced in the TAX. With the full Run 2 beam-dump data sample, NA62 is sensitive in yet unexplored regions of the dark Higgs parameter space, see Fig. 11 left, with the dark Higgs decays to ee, $\mu\mu$ and $\pi\pi$ pairs.

With the current data samples, sensitivity for unexplored regions of mixing μ in the minimal scenario is not expected. Non-minimal scenarios can be parametrized similarly to ALPs by the dark Higgs mass, lifetime and production and decay branching ratios. The model-independent bounds from Fig. 9 then apply.

For the dark Higgs portal, NA62 is significantly more competitive in the kaon mode, where a $K \to \pi S$ decay would appear as a bump above the $K^+ \to \pi^+ \nu\bar{\nu}$ spectrum. See Fig. 11 right for the exclusion in the $(m_S, \sin\theta)$ parametric space, corresponding to the full Run 1 statistics.

7. Conclusion

NA62 is a multipurpose experiment that in addition to the main goal of $K_{\pi\nu\bar{\nu}}$ and precision measurements, encompasses an extensive program dedicated to direct searches for New Physics particles in both the kaon and beam-dump modes. Recent results from NA62 have been presented,

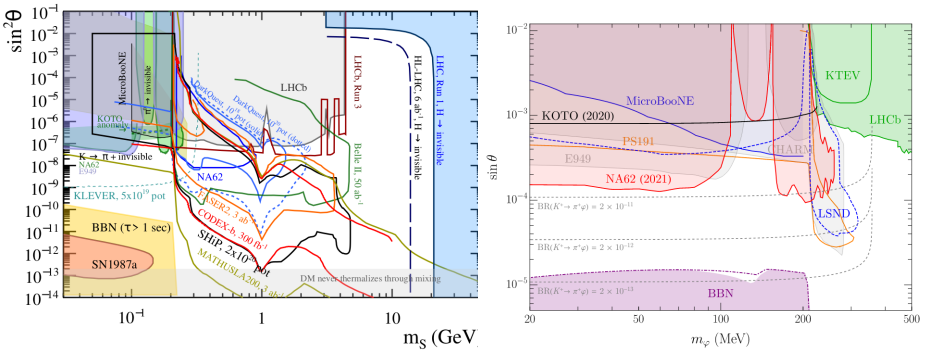

Figure 11: Sensitivity bounds in the $(m_S, \sin\theta)$ parameter space for S decaying only to visible SM particles. Left: projection for NA62 in the beam-dump mode 10^{18} POT $S \to \mu\mu$ (blue) [5]. Right: exclusion from $K^+ \to \pi^+ +$ inv. and $\pi^0 \to$ inv. decays [6] (red).

focusing on the decays of dark photons and axion-like particles into lepton pairs, utilizing the beam-dump dataset from 2021. Additionally, future prospects involving the complete Run 2 statistics and ongoing analyses with the 2021 datasets were shown.

Acknowledgments

I would like to thank the organizers of the FPCP 2023 conference for the invitation to present this summary and I want to acknowledge the support by the F.R.S.-FNRS (Fonds de la Recherche Scientifique - FNRS), Belgium, through grant FRIA/FC-36305.

References

[1] J. Beacham, C. Burrage, D. Curtin, A. De Roeck, J. Evans, J. L. Feng, C. Gatto, S. Gninenko, A. Hartin and I. Irastorza, *et al.* J. Phys. G **47** (2020) no.1, 010501 doi:10.1088/1361-6471/ab4cd2 [arXiv:1901.09966 [hep-ex]].

[2] E. Cortina Gil *et al.* [NA62], JHEP **06** (2021), 093 doi:10.1007/JHEP06(2021)093 [arXiv:2103.15389 [hep-ex]].

[3] M. Rosenthal, D. Banerjee, J. Bernhard, M. Brugger, N. Charitonidis, M. van Dijk, B. Döbrich, L. Gatignon, A. Gerbershagen and E. Montbarbon, *et al.* Int. J. Mod. Phys. A **34** (2019) no.36, 1942026 doi:10.1142/S0217751X19420260

[4] G. Anzivino, M. Barbanera, A. Bizzeti, F. Brizioli, F. Bucci, A. Cassese, P. Cenci, B. Checcucci, R. Ciaranfi and V. Duk, *et al.* JINST **13** (2018) no.07, P07012 doi:10.1088/1748-0221/13/07/P07012 [arXiv:1809.04026 [physics.ins-det]].

[5] P. Agrawal, M. Bauer, J. Beacham, A. Berlin, A. Boyarsky, S. Cebrian, X. Cid-Vidal, D. d'Enterria, A. De Roeck and M. Drewes, *et al.* Eur. Phys. J. C **81** (2021) no.11, 1015 doi:10.1140/epjc/s10052-021-09703-7 [arXiv:2102.12143 [hep-ph]].

[6] E. Goudzovski, D. Redigolo, K. Tobioka, J. Zupan, G. Alonso-Álvarez, D. S. M. Alves, S. Bansal, M. Bauer, J. Brod and V. Chobanova, *et al.* doi:10.1088/1361-6633/ac9cee [arXiv:2201.07805 [hep-ph]].

[7] B. Döbrich, J. Jaeckel, F. Kahlhoefer, A. Ringwald and K. Schmidt-Hoberg, JHEP **02** (2016), 018 doi:10.1007/JHEP02(2016)018 [arXiv:1512.03069 [hep-ph]].

[8] B. Döbrich, J. Jaeckel and T. Spadaro, JHEP **05** (2019), 213 [erratum: JHEP **10** (2020), 046] doi:10.1007/JHEP05(2019)213 [arXiv:1904.02091 [hep-ph]].

[9] B. Döbrich, F. Ertas, F. Kahlhoefer and T. Spadaro, Phys. Lett. B **790** (2019), 537-544 doi:10.1016/j.physletb.2019.01.064 [arXiv:1810.11336 [hep-ph]].

[10] J. Jerhot, B. Döbrich, F. Ertas, F. Kahlhoefer and T. Spadaro, JHEP **07** (2022), 094 doi:10.1007/JHEP07(2022)094 [arXiv:2201.05170 [hep-ph]].

[11] C. Rella, B. Döbrich and T. T. Yu, Phys. Rev. D **106** (2022) no.3, 3 doi:10.1103/PhysRevD.106.035023 [arXiv:2205.09870 [hep-ph]].